Deep–Sea Research II 205 (2022) 105183

Contents lists available at ScienceDirect

Deep-Sea Research Part II

journal homepage: www.elsevier.com/locate/dsr2

Deep carbon export peaks are driven by different biological pathways during the extended Scotia Sea (Southern Ocean) bloom

C. Manno *, G. Stowasser, S. Fielding, B. Apeland, G.A. Tarling

British Antarctic Survey, Cambridge, United Kingdom

ARTICLE INFO

Keywords:
Scotia sea
POC
$CaCO_3$
Diatoms
Faecal pellets
Sediment traps

ABSTRACT

Estimating the amount of organic carbon leaving the upper water column and becoming sequestered in the deep ocean is a major challenge in our understanding the oceanic C cycle. This study investigate deep sediment trap material collected at a 5 day resolution over a 4 month period covering the bloom in the northern Scotia Sea. This region is characterised by extensive and long-lived phytoplankton blooms that collectively take up the greatest amount of atmospheric carbon dioxide yet measured in the Southern Ocean. In particular, the study resolved multiple peaks of POC flux during the northern Scotia Sea bloom resulting from distinctly different export processes. This work also examine the contribution of diatoms and calcifying species to the POC flux as well as determining FP (faecal pellet) characteristics, including biogeochemical composition and sinking velocity. Results showed that POC flux during the bloom was concentrated in three major POC peak events. The first two POC peaks were large, of similar intensity (24.5 mg C m^{-2} d^{-1} in early November and 22.5 mg C m^{-2} d^{-1} in early December), and were dominated by faecal pellets (FPs, 60–66%). FP biogeochemical composition during these two POC peaks was characterised by a dominance of carbonate (>48%), as well as a higher sinking speed (up to 347 m d^{-1}) compared with other FP in the rest of the samples. Results suggest that the large presence of calcium carbonate in these FPs contributed to their relatively high sinking velocity which, in turn, promoted their higher level of POC export to bathypelagic depths. Intact single cell diatoms were relatively important in the first POC peak (mainly characterised by *Fragilariopsis kerguelensis* and *Thalassionema nitzschioides*), while detritus including semi-grazed phytodetritus were more abundant during the second POC peak, suggesting a change in the upper ocean C cycle between the two POC peaks. A third, smaller, POC peak (12.7 mg C m^{-2} d^{-1} in January) was dominated by diatom resting spores, mainly *Chaetoceros Hyalochaete* sp. (>70% of total diatoms contribution), which were, almost exclusively, fully intact cells. Our high resolution sampling allowed insights into short timescale processes that influence the ultimate magnitude of the substantial annual POC flux in this region. Overall our findings highlights that the temporal sequence of biological events in the surface layers during the bloom has a strong influence on both the magnitude and the composition of the fluxes.

1. Introduction

A major challenge in our understanding of the oceanic carbon cycle is estimating the amount of organic carbon that leaves the upper water column and becomes sequestered in the deep ocean (Sanders et al., 2016). The depth at which particulate organic carbon (POC) is remineralised determines the timescales over which this photosynthetically fixed CO_2 remains sequestered (Smetacek et al., 2012). Passow and Carlson (2012), for instance, considered that POC making it into the mesopelagic depth zone remains sequestered for 100 years or longer, and this timescale increases the deeper the remineralisation takes place. It follows that factors affecting the gravitational speed at which POC sinks from the upper layers, including temperature, viscosity, mineral ballasting, particle size, and composition, have a major influence on the level of sequestration. Moreover, the mean depth of remineralisation is further defined by export pathways that inject particles to depths before decomposition begins (Boyd et al., 2019). As opposed to the passive gravitational sinking of particles, on major means of particles injection is through the vertical migration of zooplankton which release their C-rich and fast sinking faecal pellets (FPs) deep in the water column. Zooplankton release FPs in both the surface and deep phases of their vertical migration and so contribute to both gravitational and particle

* Corresponding author.
E-mail address: clanno@bas.ac.uk (C. Manno).

https://doi.org/10.1016/j.dsr2.2022.105183
Received 30 March 2021; Received in revised form 20 June 2022; Accepted 8 September 2022
Available online 20 September 2022

injection pathways (Boyd et al., 2019). The relative contributions of these pathways to total POC flux varies in both space and time which, in turn, influences both the physical properties and the C content of sinking particles.

The Southern Ocean (SO) plays a dominant role in global ocean C uptake (Sarmiento et al., 1988). It supports an abundance of robust and dissolution-resistant diatoms that can escape predation after the bloom, often passing through surface layers intact and exporting their POC content to the deep ocean, as single phytoplankton cells, aggregates, or by transforming into resting spores (Boyd et al., 2000; Rembauville et al., 2015, 2018; Salter et al., 2012). Resting spores are heavily silicified cells that may further act as ballast within sinking aggregates alongside calcifying plankton that are often very abundant in the SO and can dominate carbonate fluxes (Accornero et al., 2003; Collier et al., 2000). Nevertheless, this may not always be the dominant POC export process and the repackaging of sinking cells through the release of FPs by grazing zooplankton (Cavan et al., 2015; Manno et al., 2015) as well as the production of exuvia through zooplankton moulting (Manno et al., 2020), may make an equal if not greater contribution to C export and sequestration. Hence both phytoplankton and zooplankton are crucial contributors to C export in the SO and temporal changes in their relative abundance will influence the nature and extent of the resultant POC flux.

The present study focusses on the island of South Georgia, located at the northeastern limit of the Scotia Sea, generates the largest meander in the eastward flowing ACC (Thorpe et al., 2002). In response this regional hydrography, South Georgia phytoplankton blooms develop to the northwest of the island. South Georgia's blooms regularly comprise chlorophyll *a* (chl-*a*) concentrations >10 mg m^{-3} and may be sustained for four months or more (Korb et al., 2008). Chl-concentrations first peak around November–December, with subsequent peaks between late January and April (Borrione and Schlitzer, 2013). Iron run-off from the island facilitates a spatially extensive and long-lived phytoplankton bloom (Borrione and Schlitzer, 2013) and high levels of zooplankton biomass (Atkinson et al., 2012a; Ward et al., 2012) which, together, contribute to substantial export of C to deep waters.

Our previous work in this region revealed a recurrent seasonal trend in POC flux with a high peak in the spring followed by a second, smaller POC peak, during late austral summer-early autumn (Manno et al., 2015, 2018; Rembauville et al., 2016). These POC peaks were mainly driven by large zooplankton FPs (Belcher et al., 2017; Manno et al., 2015). Nevertheless, the temporal resolution of these major flux events remains constrained by the fact that generally deep sediment traps integrate material over several weeks to months. This resolution does not allow, for instance, discrimination of how different biological pathways individually contribute to POC flux and how both the quality and quantity of particles arriving at depth alters over POC peak flux periods. High resolution insights into POC flux have particular value in helping to identify which processes within the epipelagic ecosystem have the greatest influence on determining the magnitude of the sequestration flux.

In this study, we analyse deep sediment trap material collected at a 5 d resolution over the 4 month period covering the bloom to examine (1) the quantity, type, and quality of sedimentary material, (2) the role of ecosystem structure through identifying diatoms and calcifying species and (3) the relative dominance of different POC export pathways through determining FP characteristics, including biogeochemical composition and sinking velocity. This work further compliments a simultaneous process study at the sediment trap site (P3) (Fig. 1) by the COMICS programme (this issue) during the bloom period. The COMICS programme examined a range of epipelagic and mesopelagic properties and processes at this site over 3 separate visits within a research cruise during the course of the bloom in 2017. A major focus of COMICS was on the various processes that attenuated the flux during its downward trajectory. The present work provides context in determining how much and what types of particles ultimately arrived in the deep ocean and over what timescales, and hence offers valuable insights into the importance of comparatively short time-scale processes in determining the ultimate size of the annual POC flux.

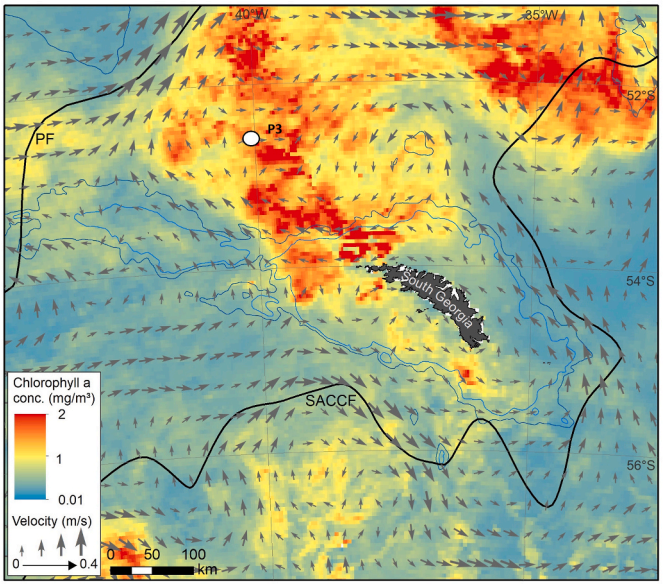

Fig. 1. Map showing the position of the P3 study site where sediment traps were moored. The background colours represent chlorophyll *a* concentration (MODIS Aqua) averaged for the study period. Grey arrows indicate altimetry-derived geostrophic velocities (AVISO), also averaged for the study period, and the thick black lines show the location of the Polar Front (PF) and Southern Antarctic Circumpolar Current Front (SACCF) (Thorpe et al., 2002). Blue isobaths are the 1000 m and 2000 m isobaths (GEBCO). The map was created by L. Gerrish, Mapping and Geographic Information Centre, BAS.

2. Methods

Sample collection- A bottom-tethered mooring was deployed at site P3 (52° 43.40′S, 40° 08.83′W; water depth 3800 m) in the north of the Scotia Sea for 12 months in December 2016 during cruise JR17002 aboard *RRS James Clark Ross* (Fig. 1). Two sediment traps (McLane Parflux sediment traps, 0.5 m^2 surface collecting area; McLane Labs, Falmouth, MA, USA) were deployed on the mooring alongside temperature/conductivity sensors (CTD SBE 37) and current meters (Aanderaa Seaguard RCM IW). Each trap contained a carousel of 21 receiving cups and was fitted with a plastic baffle mounted on the opening, to prevent the entrance of large organisms. Prior to deployment, the receiving cups were filled with sodium chloride buffered formalsaline solution (4%) to arrest biological degradation during sample collection and to avoid carbonate dissolution. The first sediment trap was deployed at 1950 m and the carousel programmed to rotate every 5 days over a 105 day period between mid-October 2017 and January 2018, covering the bloom period. The second sediment trap was deployed at a depth of 2000 m, and the sample carousel programmed to rotate at intervals of either 15 or 30 days over a 335 day period between January 2017 and January 2018. For the scope of the present study, the second sediment trap was analysed only to determine annual C flux so as to provide a context for the high temporal resolution analysis of the first trap.

Sample splitting- Once in the laboratory, the supernatant of each cup was removed by pipette and its pH was measured in order to check for possible carbonate dissolution. Prior to splitting, swimmers, i.e., zooplankton that can enter the receiving cups while alive, were carefully removed. Samples were first wet-sieved through a 1 mm nylon mesh and the remaining swimmers were hand-picked under a dissecting microscope. Large aggregates, fragments of moults and empty shell retained by the mesh were returned to the sample. Each sample was then divided

into three pseudo-replicate fractions for subsequent analysis using a McLane rotary sample splitter (McLane Labs, Falmouth, MA, USA).

Biogeochemistry analysis- Replicate fractions were vacuum filtered through pre-weighed and pre-combusted (550 °C for 5 h) GF/F filters. Filters were then desalted through briefly washing with distilled water and dried at 60 °C. Particulate organic C (POC) and total particulate C (TC) were measured by combustion in an elemental analyser (CHN, Exeter Analytical Inc. CE440 elemental analyser, accuracy ±0.15%); for POC determination, filters were pre-treated with 2 N H_3PO_4 and 1 N HCl. To estimate calcium carbonate ($CaCO_3$) particle fluxes, particulate inorganic C (PIC) was obtained by determining the difference between total particulate C (TC) and POC and multiplied by a factor of 8.33, assuming that all inorganic carbon was in the form of calcium carbonate (Accornero et al., 2003). Three blank filters were run every 25 samples.

Calcifying plankton analyses – Thecosome pteropods (hereafter 'pteropods') and foraminifera were counted and picked under a light microscope (Olympus SZX16) from three sub-sample aliquots. Specimens picked from the samples were rinsed with distilled water and air dried for 24 h. For each sample, the pteropods and foraminifera were separately combusted in a muffle furnace at 550 °C for 5 h to remove any organic carbon. After combustion, the ash was air dried and weighed on a microbalance to estimate the total amount of $CaCO_3$ attributed to pteropods and foramanifera in each sample. The coccolithophore $CaCO_3$ amount was indirectly estimated by analysing the amount of $CaCO_3$ left in the sample after the removal of pteropods and foraminifera (Manno et al., 2018). Note that this indirect estimation allowed also the inclusion of the coccolithophores contained in the FP fraction.

Diatom analyses - Diatom (including resting spores) enumeration and identification was performed using an optical microscope (Olympus BX51) following Hasle and Syvertsen (1997). An aliquot of each sample was gently homogenized and 2 mL withdrawn and diluted to a final volume of 20 mL using artificial seawater (salinity 34 PSU). Following (Rembauville et al., 2015), we used a biological counting technique that does not include any chemical treatment before counting and thereby allows the separate enumeration of full and empty cells. Cells were considered full when plasts were clearly visible and intact. Only full diatoms were considered as exporting organic matter. Full diatom and resting spores were converted to C using previously published species-specific biomass values for diatoms in this region (Rembauville et al., 2018).

Faecal Pellets analyses – FPs were counted and then classified with respect to their morphology (i.e. ovoid, spherical, and cylindrical) (González, 1992; Gonzalez and Smetacek, 1994; Manno et al., 2010). The dimensions of the first 60–100 pellets of each morphological type observed for each sample were measured (length and width) using an ocular micrometer, from which FP volume was calculated by the geometrical formulas associated with the FP shapes (González et al., 2000). Several hundred FPs were picked to investigate their biogeochemical contents in terms of $CaCO_3$, $bSiO_2$ and POC. For each station, we selected an equal number of FP for each type/shape and within each type we only selected the dominant volume range. The $CaCO_3$, POC contents within FPs were assessed following the same methodology as for biogeochemical analysis. The amount of Biogenic silica in the FPs was quantified by colorimetric analysis (Jasco UVIDEC accuracy ± 1%). bSiO2 was extracted following a progressive dissolution method in a 0.5M NaOH solution at 85 °C for 5 h (Demaster, 1991). An aliquot of each sample was taken for analysis after every hour and the relative silica data were extrapolated back to time zero to correct for the silica originating from coexisting clay minerals (Demaster, 1991).

Biogeochemical (POC, and $CaCO_3$) and biological (diatoms, FP, calcifying plankton) fluxes were expressed in mg C m^{-2} d^{-1}, estimated by dividing the total mass per sample by the time interval and the trap collection area. Please refer to supplementary material data set.

FP sinking velocity was calculated only for the two most abundant types/shape (oval and cylindrical) and for most dominant volume range (0.008–0.009 mm^3). The experiment was performed only on FPs of similar volume to allow the assessment of the influence of FP contents on sinking velocity. Potential sinking speed (m d^{-1}) was determined from FP settling velocity (cm s^{-1}), measured under controlled laboratory conditions in a cold room at 4 °C. Each FP was added to a 1 L graduated cylinder with filtered seawater (salinity 34 PSU). Each FP was placed at 100 mL under the seawater surface to avoid surface tension and allowed to sink for 100 mL (i.e. 68 mm) to attain constant velocity (Bergami et al., 2020). For each FP, the sinking velocity was calculated from the average of the time taken to sink past two marked distances (10 cm apart) (Belcher et al., 2017). Where possible, the sinking velocity of 40 FPs was determined for each sample. This measurement technique does not take into account other types of interference from the natural environment (such as temperature gradients and/or currents) and so represents a "potential" relative sinking velocity of FPs as a function of their shape, size and content.

Statistical analysis- A Kruskal–Wallis one-way ANOVA H-Test was used to determine whether there were any significant differences with regards to the different flux components and FP sinking velocity within the sampling periods, having carried out prior tests for normality and equal variance. Differences were considered significant where $p < 0.05$.

3. Results

3.1. Environmental conditions

Current meter data acquired during the sediment trap deployment suggest that sampling was not subjected to major hydrodynamic biases since mean current velocities close to the sediment traps were <12 cm s^{-1}. We therefore assumed that no substantial lateral advection occurred. Variability in current velocity and temperature was low during the sampling periods (Table 1).

3.2. POC and $CaCO_3$ flux

On annual time scale, the low resolution POC flux in P3 range between 0.42 and 11.11 mg m^{-2} d^{-1}, with relatively low values from May to Sep and maximum values in November–December (Fig. 2a). The high resolution POC flux showed a significant temporal variability between October–January, ranging from 0.78 to 24.90 mg m^{-2} d^{-1}, with two main peaks at the beginning of November and of December and a third smaller peak in January (Fig. 2b). $CaCO_3$ flux ranged between 9.91 and 74.97 mg m^{-2} d^{-1}, with the major $CaCO_3$ peaks occurring in the same periods as the first two POC peaks, but no subsequent $CaCO_3$ peak corresponding to the third smaller POC peak (Fig. 2c). Overall, POC flux in October–January represented 82.13% of the annual flux of POC for the study period.

3.3. POC and $CaCO_3$ components

FPs dominated the total POC flux in the first two peaks, while diatoms dominated the third minor peak in January, being the major contributor POC flux throughout the wider latter period (Fig. 3a) (Kruskal–Wallis one-way analysis of variance (ANOVA), FP, $H = 8.43$, $p < 0.05$; Diatoms $H = 7.60$ $p < 0.05$; Detritus $H = 10.09$ $p < 0.05$). The relative contribution of the different calcifiers to total $CaCO_3$ flux varied between each sampling period. The first $CaCO_3$ peak was mainly driven

Table 1
Average of Current Speed (CS) expressed in cm s^{-1} and Temperature (T) expressed in °C. SD is Standard Deviation.

	Nov	Dec	Jan	Oct–Jan
CS cm s^{-1}	7.03	7.34	9.24	6.79
SD (±)	3.23	3.85	3.49	4.22
T °C	0.51	0.36	0.45	0.43
SD (±)	0.34	0.11	0.06	0.22

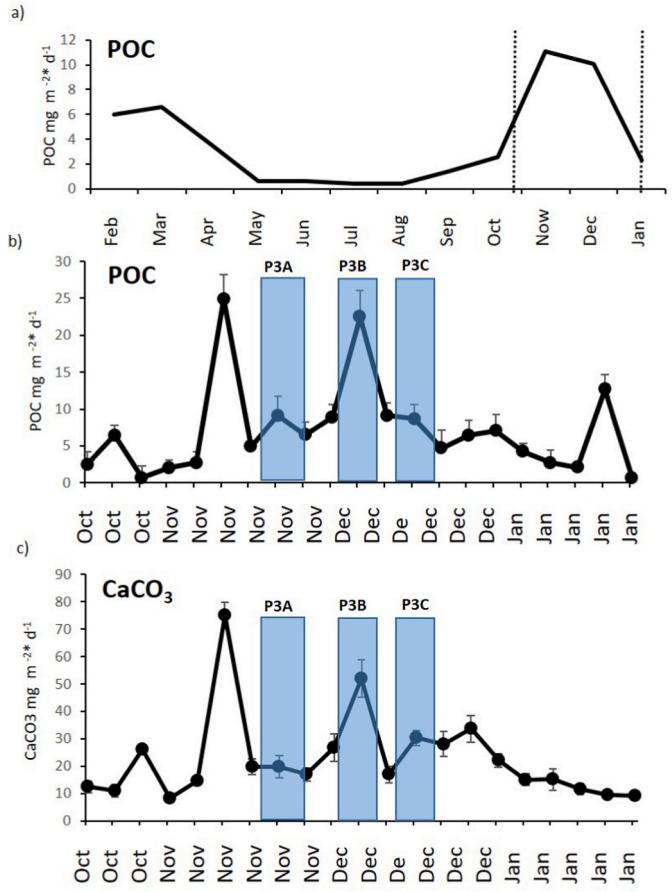

Fig. 2. Variability of flux material expressed as mg m^{-2} d^{-1} from samples collected by the sediment trap deployed at P3 **a)** annual trend of Particulate Organic Carbon (POC), 2000 m; **b)** POC high resolution trend (Oct–Jan), 1950 m; **c)** Calcium Carbonate ($CaCO_3$) high resolution trend (Oct–Jan), 1950 m. Region between the dashed lines in **a)** represents the corresponding period in **b)** and **c)**. Light blue columns indicate the period when COMICS cruise DY086 visited the site (over three visits: P3A, P3B, P3C). Error bars indicate standard deviation.

by pteropods while coccolithophores were a secondary contributor (Fig. 3b). Pteropods and coccolithophores made an almost equal contribution to the second $CaCO_3$ peak. Peropods represent the non-FP fraction of the flux while coccolithophores include both the FP and non-FP fraction of the flux. The contribution from foraminifera was comparatively low and less variable over the entire sampling period and became comparatively more important at the end of the sampling period.

3.4. Diatom assemblage

The diatom assemblage was mainly dominated by *Fragilariopsis kerguelensis* and *Thalassionema* spp *(mainly T. nitzschioides)* from October to the last week of December, together accounting for >82% of total diatom abundance. Other taxa *(i.e. Eucampia antarctica, Navicula* sp.) made further small contributions. After this period, diatom resting spores (mainly *Chaetoceros (subgenus) Hyalochaete* sp.*)* became increasingly important (up to 70% of total diatom abundance) (Fig. 4 a). Most diatoms within the sediment trap samples were empty but the amount of full diatoms increased in January due to the presence of these resting spores (Fig. 4b). It is also notable that an increase in the full/empty frustule ratio occurred in November (during the first POC flux peak) where full diatoms contributed up to 40% of the total diatom assemblage.

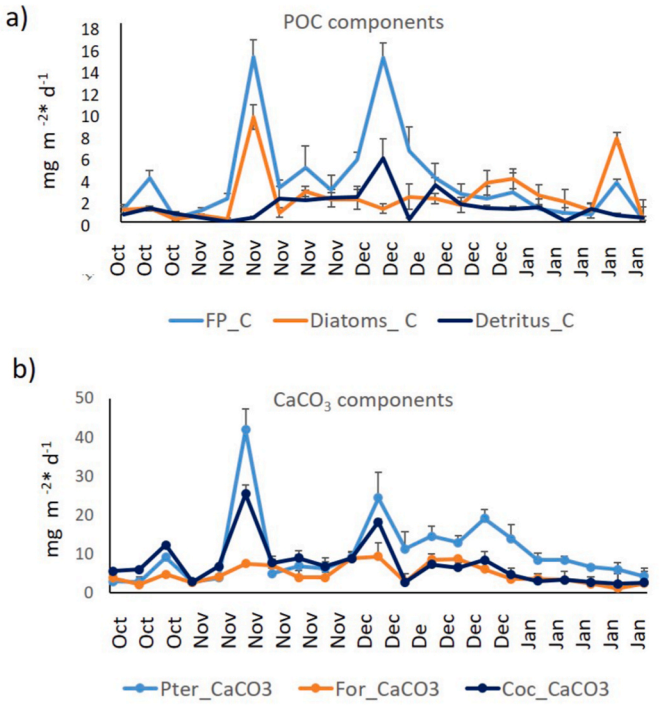

Fig. 3. Contribution (expressed as mg m^{-2} d^{-1}) of **a)** FP, diatoms and detritus to POC flux; **b)** calcifying organisms (i.e. foraminifera, pteropods, coccolithophores) to the $CaCO_3$ flux, from samples collected by the high temporal resolution sediment trap deployed at 1950 m at P3 during the 2017/18 bloom. Error bars indicate standard deviation.

3.5. FP assemblage, biogeochemical composition and sinking velocity

The distribution of FP shapes did not change between the POC peaks, with oval and cylindrical types always dominating (Fig. 5a). Over the entire period, oval, cylindrical and spherical FPs contributed 56%, 35% and 8% of the total FP assemblage respectively.

FP biogeochemical composition was, in general, dominated by $bSiO_2$ (up to 66%) (Fig. 5b), except for the first and second peak flux periods where FP composition was mainly dominated by $CaCO_3$ (48% and 43%, respectively). POC made up 22–27% of the total biogeochemical composition of FPs throughout the study period except during the last two weeks of January, where it increased to 40%.

FPs volume ranged between 0.003 and 0.04 mm^3, with the most abundant FPs being between 0.008 and 0.009 mm^3 (comprising 40% of all FPs). Across all FP volume, oval FPs were the dominant type, followed by cylindrical and then spherical (Fig. 6a).

FP sinking velocity was very similar between the two FP types and ranged from 255 to 347 m d^{-1} for oval FPs and 236–335 m d^{-1} for cylindrical FPs. For both FP types, sinking velocities were significantly higher during peak flux periods (oval $H = 6.7$ $p < 0.01$, cylindrical H8.9 $p < 0.01$) (Fig. 6b).

4. Discussion

At the P3 study site, POC maximum flux we observed (25 mg m^{-2} d^{-1}) was the same order of magnitude as previous observations in this region (Manno et al., 2015; Rembauville et al., 2016; POC flux up to 23 mg m^{-2} d^{-1}), and other iron-fertilized sites in the Southern Ocean (Rembauville et al., 2015; Salter et al., 2012; POC flux up to 27 mg m−2 d−1). POC flux during the bloom represented 82% of the total annual POC flux with a significant fraction (40%) occurring during three peak flux events. The composition of fluxed material differed distinctly between each of those events. While the first two POC peaks were dominated by FPs, the last was mainly driven by diatom resting spores. Our

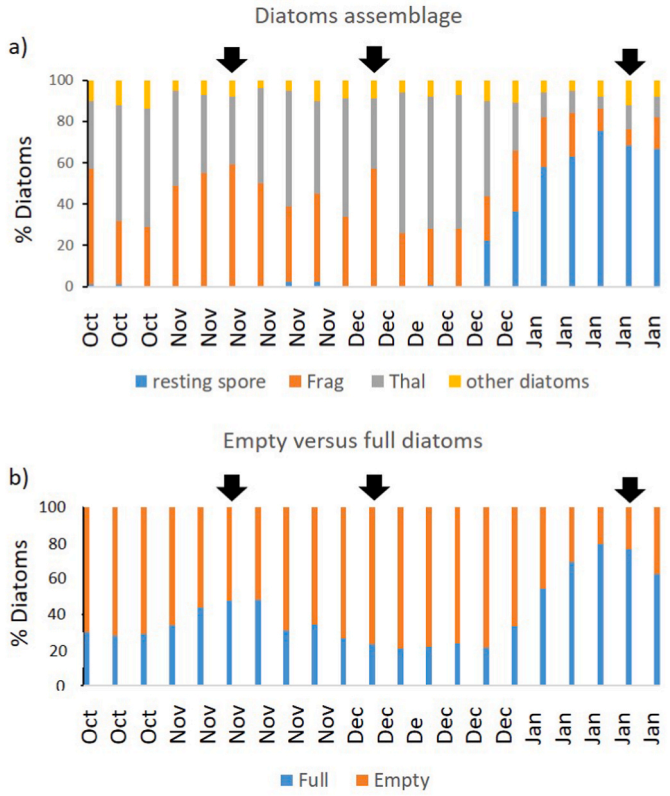

Fig. 4. a) contribution (expressed as % of total abundance) of resting spores, *Fragilariopsis kerguelensis* (Frag), *Thalassionema nitzschioides* (Thal) and other diatoms to the diatom assemblage captured by the high resolution sediment trap deployed at 1950 m at P3 during the 2017/18 bloom **b)** Full versus empty diatoms (expressed as % of total abundance). Black arrows indicate the timing of peak POC flux events.

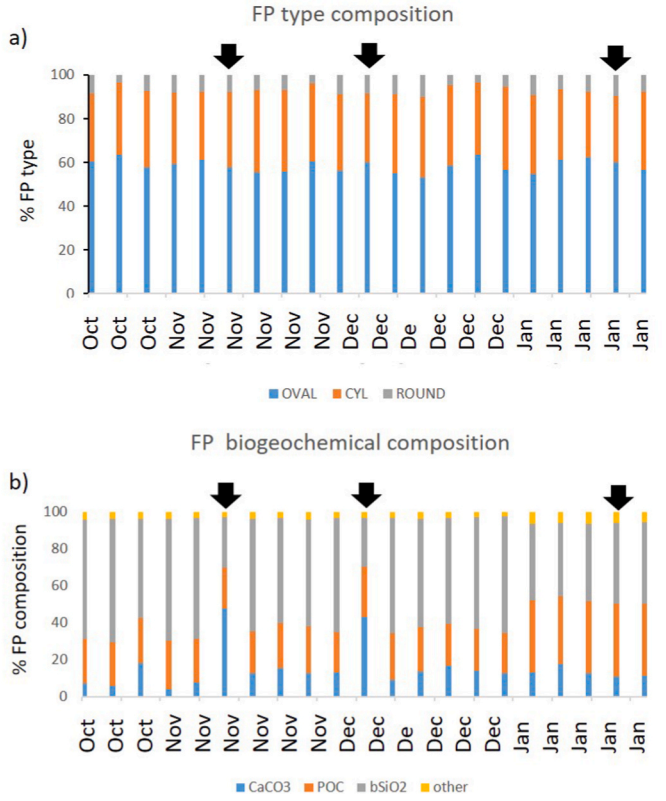

Fig. 5. a) types (expressed as % of the total abundance) and **b)** biogeochemical composition (expressed as % in terms of relative weight) with regards $CaCO_3$, POC, $bSiO_2$ and other components from samples collected by the sediment trap deployed at 1950 m at P3 during the 2017/18 bloom. Black arrows indicate the timing of peak POC flux events.

results suggest that, over the period of the bloom, most POC flux occurred in short bursts of periods of less than 10 days. Such short-lived events are difficult to capture through ship-based oceanographic sampling. For instance, while the COMICS cruise DY086 visited the P3 site three times over a 35 day period (Fig. 1), the first POC peak flux occurred before of the first visit (P3A), the second took place during second visit (P3B) and the third sometime after the last visit (P3C). This emphasises the value of combining different sampling approaches to gain a full oversight of the time-course of POC flux.

4.1. Role of FPs as vectors of POC

The two largest POC peak flux periods, in early November (23 mg $m^{-2}\,d^{-1}$) and early December (22 mg $m^{-2}\,d^{-1}$), were both driven by FPs which contributed 60% and 66% to total POC flux respectively. The critical role of FPs as a vector in the downward transport of carbon in the Scotia Sea has already been highlighted in previous studies (Belcher et al., 2017; Liszka et al., 2019; Manno et al., 2015, 2020). Usually sinking velocity of FPs (e.g. Atkinson et al., 2012b, Belcher et al., 2017) can be more than one order of magnitude higher than diatoms (0.7–30 m d^{-1}; e.g. Gemmell et al., 2016; Passow, 1991; Miklasz and Denny, 2010). However, our quantification of the relative biogeochemical contents of FPs, and the ways these affect sinking speed, represent a new level of understanding of how this flux is modulated. In the present study, we found that the biogeochemical composition of FPs during the two major POC peak flux periods differed from that found at other times during the study period. Specifically, during both the early November and early December POC peaks, carbonate was the dominant biogeochemical component of FPs while biogenic silica dominated at other times.

Furthermore, FP sinking velocity during the two largest POC peaks (320–347 m d^{-1}) was 19% higher than at other times. It has previously been recognised that diatom silica frustules tend to produce denser, faster-sinking FPs (i.e. Ploug et al., 2008). Here we suggest that the large presence of carbonate in these FPs, which has a molecular weight higher than particulate biogenic silica, is responsible for their relatively high sinking velocity which, in turn, promotes a higher level of export to bathypelagic depths. We can assume that the residual amount of material (<5% overall the samples) in the FP was made up of lithogenic content. However since the amount was relatively small and had a low variability over the study period (e.g. 2<x<5%) we can assume that the relative influence of this material as ballast within the FPs was almost negligible. A further feature of FPs was that FPs samples with high (and similar) % $CaCO_3$ content grouped together with FPs with high (and similar) sinking velocity, and the rest of the Fps samples having lower (but variable) % $CaCO_3$ content grouped together with relatively lower (and less variable) sinking velocity (Fig. 7b). This feature was observed for both the oval and cylindrical types of FP (Fig. 7b). This observation highlights that, with regards to the export potential of FPs, when size is similar, it is the contents and not the shape of the FP that matters most. Previous study showed that ballasting from carbonate aggregate resulted in higher sinking velocities than aggregates ballasted by opal (Iversen and Ploug, 2010). Further (Laurenceau-Cornec, 2015), observed a correlation of particle sinking velocity with size only within homogeneous sources of aggregates. While an FP that is filled with $CaCO_3$ contains less POC, such FPs have a greater sinking velocity and hence chance of making it to depth. Our observations further suggest that, even though amount of POC per FP is relatively low (Fig. 5b), this greater export efficiency and transfer might explain the higher POC flux

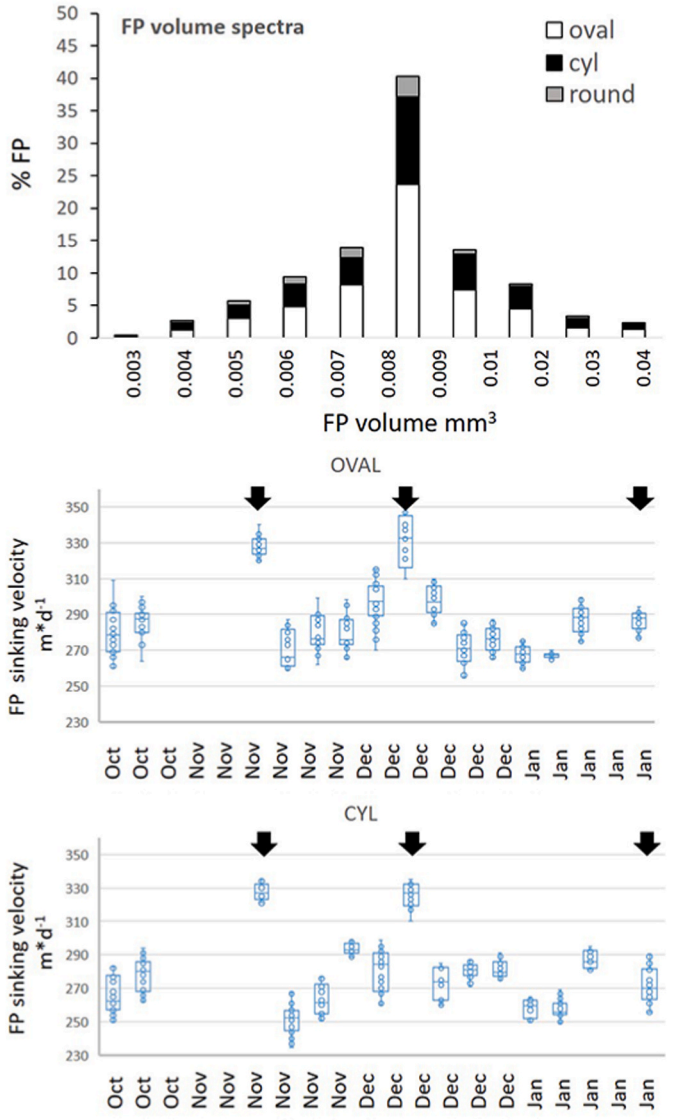

Fig. 6. a, Faecal pellet class volume abundance and relative contribution for each faecal pellet type (i.e. oval, round, cylindrical) **b**, Faecal pellet sinking rates (expressed as m d^{-1}), oval (top), cylindrical (bottom) from samples collected by the high resolution sediment trap deployed at 1950 m at P3 during the 2017/18 bloom.

observed during the bloom period in November and December (Fig. 2).

The dominant biogeochemical FP content within flux peaks match well with the dominant biological components of the flux during these events (e.g. calcifiers versus diatoms). This observation suggest that FPs content is a function of the community structure present in the water column. In particular, a dominance of carbonates within FPs corresponds well with peaks of CaCO3 flux generated by calcifying plankton in sediment trap samples (Fig. 7a). Both shelled pteropods and coccolithophores strongly contribute to the calcium carbonate peaks (up to 56% and 36% respectively), with foraminifera making a further minor contribution (up to 18%). Periods when pteropods but not coccolithophores were abundant in sediment trap samples, such as during the second week of December and in January, did not correspond to periods when carbonate content within FPs was also high. This observation is in agreement with previous work by Manno et al. (2018) in the same region, who found that carbonate content of FPs was mainly of coccolithophore origin. Despite the fact that single-celled coccolithophores are commonly associated with low POC flux (Klaas and Archer, 2002), this is not the case when they become repackaged in FPs and enhance export efficiency through acting as ballast. Conversely, pteropod shells are too large to be consumed by mesozooplankton. Furthermore, pteropods within our sediment trap samples were mainly empty shells suggesting that their organic contents had been ingested during predation and their carbonate shells had not been consumed for subsequent egestion in FPs. Empty shells are often generated through predation activity by gymnosomatous (non-shelled) pteropods such as *Clione* spp., who feed almost exclusively on shelled pteropods, using tentacles to grab the shell and extract the soft body tissue (Conover and Lalli, 1972).

4.2. Role of diatoms and organic detritus as vectors of POC

We found that, during the first peak in November, single cell diatoms made a substantial contribution to POC flux (39%). The diatom assemblage was dominated by intact cells of *F. kerguelensis* and *T. nitzschioides* which have robust and heavily silicified silicified frustules. Previous studies investigating the diatom assemblage in the water column in this region (Korb et al., 2012) show variance between seasons with a dominance of weakly and heavily silicified diatoms in the early spring and summer-autumn season respectively (e.g. M. *adele*, C. *pennatum,* T. *nitzschoides* and Fragilariopsis spp). In this study, the dominance of *F. kerguelensis* and *T. nitzschioides* in the sediment trap during Nov–Dec, highlights preferential export of high siliceous species to the deep ocean.

Conversely, in the second POC peak at the beginning of December, contributed more than single cell diatoms contributed less than organic detritus (e.g. fragments of organic tissue, moults, FPs, and semi-grazed phytodetritus) (5% vs 28% respectively), suggesting a biological shift in the surface ocean. Surface ocean samples collected during the COMICS cruise showed a high abundance of diatoms (all >20 μm) with *Chaetoceros* spp., *Thalassionema nitzschioides*, *Fragilariopsis kerguelensis*, *Eucampia antarctica*, and *Pseudo-nitzschia* spp as common taxa) during their first visit (15–22 Nov) just after the first flux POC peak (Ainsworth et al., this issue) as well as high export fluxes mean: 646 mg C m^2 d^{-1} at 95 m depth; Giering et al., this issue) that were likely associated with large diatoms (based on in situ imaging; González et al., 2000 and pers. comm.). This period was identified as a surface bloom, with the two following visits (P3B: 29 Nov – 6 Dec and P3C: 9–16 Dec) capturing the bloom decline, which was associated with a decrease in diatom biomass (Ainsworth et al., 2022, this issue), a decrease in export flux (409 and 287 mg C m^2 d^{-1} at 95 m depth, respectively; Giering et al., this issue) and a decrease in the carbon flux measured in the deep sediment trap in mid-December (down to 10 mg C m^2 d^{-1}, Fig. 2, this study). The surface observations hence match the deep sediment trap observations with a shift from diatom-mediated export to export associated with partly recycled material. It is important, however, to keep in mind that only a small fraction of exported material will reach the deep sediment traps at 2000 m. Villa-Alfageme et al. (this issue) found that, during the COMICS occupation, the average sinking velocity of particles at the base of the euphotic zone was <60 m d^{-1} (and increased consistently with depth <120 m d^{-1}at 450m) implying that the majority of particles would take >1–2 weeks to reach sediment trap depth. Small detritus fragments and FPs tend to be re-mineralised within the mesopelagic layer soon after production, as observed in previous work in this region (Liszka et al., 2019). Consequently, only the larger detritus fragment and FPs are likely to contribute to the deep POC fluxes. This suggestion is also supported by the observation that small FPs (<0.003 mm^3, mainly produced by copepods), though produced in high numbers, are poorly exported and rarely reach the bathypelagic (Belcher et al., 2017). Indeed, we found that only 2% of FPs collected in the sediment trap were smaller than 0.003 mm^3. However, we cannot exclude that the variability between the intensity of intact diatoms and detritus fragments within the sinking material might also be indicative of different grazing pressures between the two peak flux events. Thus another alternative explanation might be that grazing pressure during the second peak was higher but generated damaged diatoms through messy feeding (Mayor et al., 2014) which

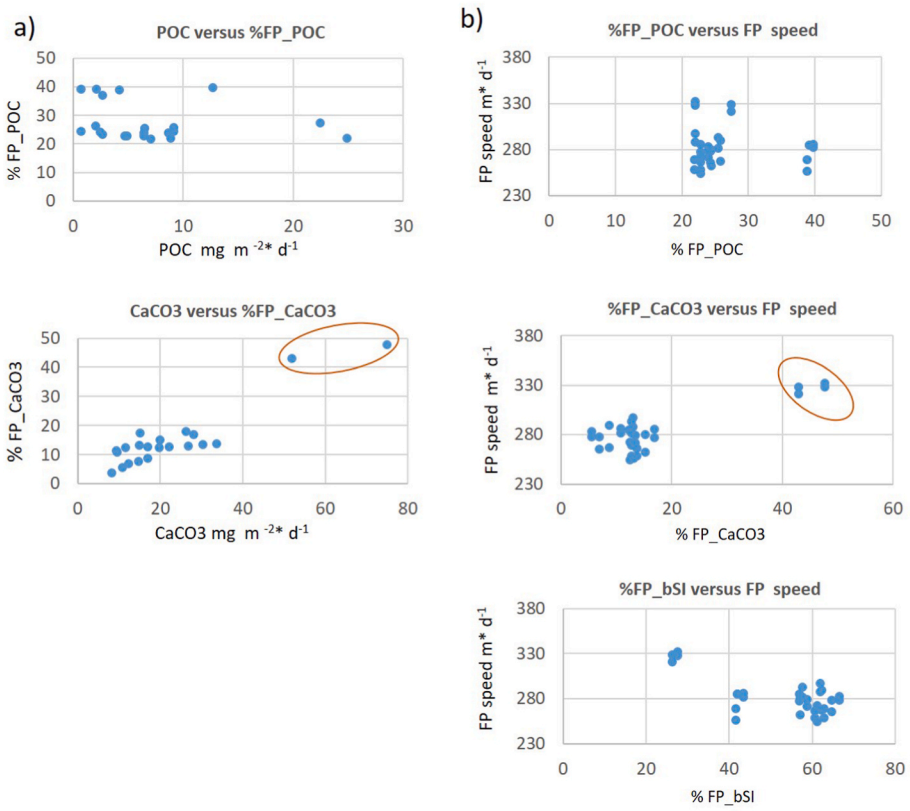

Fig. 7. Relationship of **a)** POC (mg C m^{-2} d^{-1}) and POC (mg C m^{-2} d^{-1}) versus % of POC and $CaCO_3$ contents in the FPs (FP_POC, FP_$CaCO_3$); **b)** % of contents in the FPs (FP_POC, FP_$CaCO_3$ and FP_bSi_2) versus FP sinking speed (m d^{-1}).

subsequently formed detritus fragment.

4.3. Role of resting spores as vectors of POC

We observed another small flux peak (12 mg m^{-2} d^{-1}) at the beginning of the last week of January which was characterised by a dominance of diatom resting spores (68%), mainly Chaetoceros (subgenus) Hyalochaete sp. These resting spores were almost exclusively exported as fully intact cells. Despite diatoms having been linked with high POC flux and low efficiency POC export (Armstrong et al., 2001) this is not the case when they are in the form of resting spores (Rembauville et al., 2016; Salter et al., 2012). Spore formation leads to protection from grazing through the acquisition of heavily silicified valves making them a less accessible food source and less prone to remineralisation and repackaging. Resting stages are generally produced when environmental conditions are not optimal for growth. The important role of diatoms resting spores as a POC vector to the bathypelagic has been reported previously in this region (Rembauville et al., 2018) as well as in the other naturally iron-fertilized Southern Ocean islands (i.e. Kerguelen, Rembauville et al., 2016; and Crozet, Salter et al., 2012). Our study area is characterised by a decrease in nutrient availability in summer (Korb et al., 2008; Nielsdóttir et al., 2012) suggesting that diatoms revert to this life stage at the onset of nutrient limitation in early summer. In particular, silicic acid depletion can be substantial, with concentrations near South Georgia reduced from winter values of >30 mmol m^{-3} to <1 mmol m^{-3} by January (Whitehouse et al., 2000). While our data do not allow us to understand why spore formation was initiated, nutrient availability in the epipelagic zone was found to decrease from November to January during present study period (silicate dropped by ~1–2 uM and nitrate by ~1–2 uM; Ainsworth et al., this issue). Furthermore, despite the fact that the resting spores of *Chaetoceros* dominated the third peak flux event, it was not the dominant phytoplankton species in sediment trap samples overall. Neither does this species dominate the active phytoplankton community in the epipelagic in this region (Korb et al., 2012). This observation is in agreement with the study of Rynearson et al. (2013), which emphasises how non-dominant species of phytoplankton community during a transient life stage (such as resting spores) can contribute more to carbon flux than their more abundant counterparts.

5. Conclusion

Settling material collected by a deep sediment trap reveals how short time-scale processes are the major influence on POC flux in the northern sector of the Scotia Sea. The high temporal resolution of our sampling design enabled us to detect multiple peaks of POC flux over the duration of the bloom period, which would otherwise have remained unresolved with more standard sampling designs. Our results highlight that similar magnitudes of POC flux in the deep ocean (i.e. first and second peak fluxes) may be generated by multiple different biological processes and interactions in the surface layers. In particular, our findings show that fast sinking FPs characterised by high $CaCO_3$ content dominate the POC peaks in November and December. The contribution of diatoms changed between peak flux events with a dominance of single intact cells in November, semi-grazed phytodetritus in December and resting spores in January. Overall, this study emphasises the role of life cycles and trophic interactions in conditioning the flux of POC. Furthermore, the temporal sequence of biological events in the surface layers has a strong influence on both the magnitude and composition of the fluxes that eventually become sequestered. We advocate that studies combining water column environmental conditions and high resolution sediment trap data are essential for progressing our understanding of how ecosystem structure and dynamics drive the processes that control POC export in the Scotia Sea.

Author Statement

Clara Manno: Conceptualization, Methodology, Writing – original draft, Investigation. Sophie Fielding, Gabi Stowasser: investigation. Geraint A. Tarling: Supervision, funding acquisition, Sophie Fielding, Gaby Stowasser, Geraint A. Tarling: Writing- Reviewing and Editing, fieldwork participation, Bjorg Apeland: Resources

Declaration of competing interest

The authors declare that they have no known competing financial interests or personal relationships that could have appeared to influence the work reported in this paper.

Acknowledgements

We thank the captain, officers and the crew of the RRS James Clark Ross for their support in all the logistical operations on board, and we also thank the Antarctic Logistics and Infrastructure programme at British Antarctic Survey, and Peter Enderlein for support of the deployment and recovery of the mooring and Paul Geissler for facilitates CHN analyses. We thank Federico Giglio (ISP-CNR) for the help with Biosilica components. Clara Manno time was supported by UKRI FLF project MR/T020962/1. We thanks the anonymous reviewers for their careful reading of our manuscript and their many insightful comments. This work was carried out as part of the Ecosystems programme WCB-POETS surveys and the Scotia Sea Open Ocean Laboratories (SCOOBIES) sustained observation programme at the British Antarctic Survey.

Appendix A. Supplementary data

Supplementary data to this article can be found online at https://doi.org/10.1016/j.dsr2.2022.105183.

References

Accornero, A., Manno, C., Esposito, F., Gambi, M.C., 2003. The vertical flux of particulate matter in the polynya of Terra Nova Bay. Part II. Biological components. Antarct. Sci. 15, 175–188. https://doi.org/10.1017/S0954102003001214.

Ainsworth, J., Poulton, A.J., Lohan, M.C., Stinchcombe, M.C., Lough, A.J.M., Moore, C. M., Iron cycling during the decline of a South Georgia Bloom. Deep-Sea Research, 2022. Iron cycling during the decline of a South Georgia Bloom. Deep-Sea Research. (this issue).

Armstrong, R.A., Lee, C., Hedges, J.I., Honjo, S., Wakeham, S.G., 2001. A new, mechanistic model for organic carbon fluxes in the ocean based on the quantitative association of POC with ballast minerals. Deep Sea Res. Part II Top. Stud. Oceanogr. 49, 219–236. https://doi.org/10.1016/S0967-0645(01)00101-1.

Atkinson, A., Ward, P., Hunt, B.P.V., Pakhomov, E.A., Hosie, G.W., 2012a. An overview of Southern Ocean zooplankton data: abundance, biomass, feeding and functional relationships. CCAMLR Sci. 19, 171–218.

Atkinson, A., Schmidt, K., Fielding, S., Kawaguchi, S., Geissler, P.A., 2012b. Variable food absorption by Antarctic krill: relationships between diet, egestion rate and the composition and sinking rates of their fecal pellets. Deep Sea Res. Part II Top. Stud. Oceanogr. 59, 147–158.

Belcher, A., Manno, C., Ward, P., Henson, S., Sander, R., Tarling, G.A., 2017. Copepod faecal pellet transfer through the meso- and bathypelagic layers in the Southern Ocean in spring. Biogeosciences 14, 1511–1525. https://doi.org/10.5194/bg-14-1511-2017.

Bergami, E., Manno, C., Cappello, S., Vannuccini, M.L., Corsi, I., 2020. Nanoplastics affect moulting and faecal pellet sinking in Antarctic krill (Euphausia superba) juveniles. Environ. Int. 143, 105999 https://doi.org/10.1016/j.envint.2020.105999.

Borrione, I., Schlitzer, R., 2013. Distribution and recurrence of phytoplankton blooms around South Georgia, Southern Ocean. Biogeosciences 10, 217–231. https://doi.org/10.5194/bg-10-217-2013.

Boyd, P.W., Claustre, H., Levy, M., Siegel, D.A., Weber, T., 2019. Multi-faceted particle pumps drive carbon sequestration in the ocean. Nature 568, 327–335. https://doi.org/10.1038/s41586-019-1098-2.

Boyd, P.W., Watson, A.J., Law, C.S., Abraham, E.R., Trull, T., Murdoch, R., Bakker, D.C. E., Bowie, A.R., Buesseler, K.O., Chang, H., Charette, M., Croot, P., Downing, K., Frew, R., Gall, M., Hadfield, M., Hall, J., Harvey, M., Jameson, G., LaRoche, J., Liddicoat, M., Ling, R., Maldonado, M.T., McKay, R.M., Nodder, S., Pickmere, S., Pridmore, R., Rintoul, S., Safi, K., Sutton, P., Strzepek, R., Tanneberger, K., Turner, S., Waite, A., Zeldis, J., 2000. A mesoscale phytoplankton bloom in the polar Southern Ocean stimulated by iron fertilization. Nature 407, 695–702. https://doi.org/10.1038/35037500.

Cavan, E.L., Le Moigne, F.A.C., Poulton, A.J., Tarling, G.A., Ward, P., Daniels, C.J., Fragoso, G.M., Sanders, R.J., 2015. Attenuation of particulate organic carbon flux in the Scotia Sea, Southern Ocean, is controlled by zooplankton fecal pellets. Geophys. Res. Lett. 42, 821–830. https://doi.org/10.1002/2014GL062744.

Collier, R., Dymond, J., Honjo, S., Manganini, S., Francois, R., Dunbar, R., 2000. The vertical flux of biogenic and lithogenic material in the Ross Sea: moored sediment trap observations 1996–1998. Deep Sea Res. Part II Top. Stud. Oceanogr. 47, 3491–3520. https://doi.org/10.1016/S0967-0645(00)00076-X.

Conover, R.J., Lalli, C.M., 1972. Feeding and growth in Clione limacina (Phipps), a pteropod mollusc. J. Exp. Mar. Biol. Ecol. 9, 279–302. https://doi.org/10.1016/0022-0981(72)90038-X.

Demaster, D.J., 1991. Measuring biogenic silica in marine sediments and suspended matter. In: Marine Particles: Analysis and Characterization. American Geophysical Union (AGU), pp. 363–367. https://doi.org/10.1029/GM063p0363.

Gemmell, B.J., Oh, G., Buskey, E.J., Villareal, T.A., 2016. Dynamic sinking behaviour in marine phytoplankton: rapid changes in buoyancy may aid in nutrient uptake. Proc. R. Soc. B Biol. Sci. 283, 20161126 https://doi.org/10.1098/rspb.2016.1126.

Giering S.L.C., Lampitt R.S., Iversen M.H., Saw K., Carvalho F., Briggs N., Kiriakoulakis K., Preece C., Wolff G., Parbotsava K., East H., Peele K., Pebody C., Villa-Alfageme M., Espinola B., Henson S.A., Stinchcombe M., Klawonn I., Sanders R. (this issue) POC carbon stocks and fluxes during a phytoplankton bloom near South Georgia (COMICS1).

González, H.E., 1992. The distribution and abundance of krill faecal material and oval pellets in the Scotia and Weddell Seas (Antarctica) and their role in particle flux. Polar Biol. 12, 81–91. https://doi.org/10.1007/BF00239968.

González, H.E., Ortiz, V.C., Sobarzo, M., 2000. The role of faecal material in the particulate organic carbon flux in the northern Humboldt Current, Chile (23°S), before and during the 1997–1998 El Niño. J. Plankton Res. 22, 499–529. https://doi.org/10.1093/plankt/22.3.499.

Gonzalez, H.E., Smetacek, V., 1994. The possible role of the cyclopoid copepod Oithona in retarding vertical flux. PoLAR 113, 233–246.

Hasle, G.R., Syvertsen, E.E., 1997. Marine diatoms. In: Tomas, C.R. (Ed.), Identifying Marine Phytoplankton. Academic Press, London and New York, pp. 5–385. Elsevier.

Iversen, M.H., Ploug, H., 2010. Ballast minerals and the sinking carbon flux in the ocean: carbon-specific respiration rates and sinking velocity of marine snow aggregates. Biogeosciences 7, 2613–2624.

Klaas, C., Archer, D.E., 2002. Association of sinking organic matter with various types of mineral ballast in the deep sea: implications for the rain ratio. Global Biogeochem. Cycles 16, 14–63. https://doi.org/10.1029/2001GB001765.

Korb, R.E., Whitehouse, M.J., Atkinson, A., Thorpe, S.E., 2008. Magnitude and maintenance of the phytoplankton bloom at South Georgia: a naturally iron-replete environment. Mar. Ecol. Prog. Ser. 368, 75–91.

Korb, R.E., Whitehouse, M.J., Ward, P., Gordon, M., Venables, H.J., Poulton, A.J., 2012. Regional and seasonal differences in microplankton biomass, productivity, and structure across the Scotia Sea: implications for the export of biogenic carbon. Deep Sea Res. Part II Top. Stud. Oceanogr. 59–60, 67–77. https://doi.org/10.1016/j.dsr2.2011.06.006.

Laurenceau-Cornec, E.C., 2015. The relative importance of phytoplankton aggregates and zooplankton fecal pellets to carbon export: insights from free-drifting sediment trap deployments in naturally iron-fertilised waters near the Kerguelen Plateau. Biogeosciences 12, 1007–1027.

Liszka, C.M., Manno, C., Stowasser, G., Robinson, C., Tarling, G.A., 2019. Mesozooplankton community composition controls faecal pellet flux and remineralisation depth in the Southern Ocean. Front. Mar. Sci. 6, 1–14. https://doi.org/10.3389/fmars.2019.00230.

Manno, C., Fielding, S., Stowasser, G., Murphy, E.J., Thorpe, S.E., Tarling, G.A., 2020. Continuous moulting by Antarctic krill drives major pulses of carbon export in the north Scotia Sea, Southern Ocean. Nat. Commun. 11, 6051. https://doi.org/10.1038/s41467-020-19956-7.

Manno, C., Giglio, F., Stowasser, G., Fielding, S., Enderlein, P., Tarling, G.A., 2018. Threatened species drive the strength of the carbonate pump in the northern Scotia Sea. Nat. Commun. 9, 4592. https://doi.org/10.1038/s41467-018-07088-y.

Manno, C., Stowasser, G., Enderlein, P., Fielding, S., Tarling, G.A., 2015. The contribution of zooplankton faecal pellets to deep-carbon transport in the Scotia Sea (Southern Ocean). Biogeosciences 12, 1955–1965. https://doi.org/10.5194/bg-12-1955-2015.

Manno, C., Tirelli, V., Accornero, A., Fonda Umani, S., 2010. Importance of the contribution of Limacina helicina faecal pellets to the carbon pump in Terra Nova Bay (Antarctica). J. Plankton Res. 32, 145–152. https://doi.org/10.1093/plankt/fbp108.

Mayor, D.J., Sanders, R., Giering, S.L.C., Anderson, T.R., 2014. Microbial gardening in the ocean's twilight zone: detritivorous metazoans benefit from fragmenting, rather than ingesting, sinking detritus. Bioessays 36, 1132–1137. https://doi.org/10.1002/bies.201400100.

Miklasz, K.A., Denny, M.W., 2010. Diatom sinkings speeds: improved predictions and insight from a modified Stokes' law. Limnol. Oceanogr. 55 (6), 2513–2525.

Nielsdóttir, M.C., Bibby, T.S., Moore, C.M., Hinz, D.J., Sanders, R., Whitehouse, M., Korb, R., Achterberg, E.P., 2012. Seasonal and spatial dynamics of iron availability in the Scotia Sea. Mar. Chem. 130–131, 62–72. https://doi.org/10.1016/j.marchem.2011.12.004.

Passow, U., 1991. Species-specific sedimentation and sinking velocities of diatoms. Mar. Biol. 108, 449–455. https://doi.org/10.1007/BF01313655.

Passow, U., Carlson, C.A., 2012. The biological pump in a high CO2 world. Mar. Ecol. Prog. Ser. 470, 249–271. https://doi.org/10.3354/meps09985.

Ploug, H., Iversen, M.H., Fischer, G., 2008. Ballast, sinking velocity, and apparent diffusivity within marine snow and zooplankton fecal pellets: implications for

substrate turnover by attached bacteria. Limnol. Oceanogr. 53, 1878–1886. https://doi.org/10.4319/lo.2008.53.5.1878.

Rembauville, M., Blain, S., Manno, C., Tarling, G., Thompson, A., Wolff, G., Salter, I., 2018. The role of diatom resting spores in pelagic–benthic coupling in the Southern Ocean. Biogeosciences 15, 3071–3084. https://doi.org/10.5194/bg-15-3071-2018.

Rembauville, M., Manno, C., Tarling, G.A., Blain, S., Salter, I., 2016. Strong contribution of diatom resting spores to deep-sea carbon transfer in naturally iron-fertilized waters downstream of South Georgia. Deep-Sea Res. Part I Oceanogr. Res. Pap. 115, 22–35. https://doi.org/10.1016/j.dsr.2016.05.002.

Rembauville, M., Salter, I., Leblond, N., Gueneugues, A., Blain, S., 2015. Export fluxes in a naturally iron-fertilized area of the Southern Ocean – Part 1: seasonal dynamics of particulate organic carbon export from a moored sediment trap. Biogeosciences 12, 3153–3170. https://doi.org/10.5194/bg-12-3153-2015.

Rynearson, T.A., Richardson, K., Lampitt, R.S., Sieracki, M.E., Poulton, A.J., Lyngsgaard, M.M., Perry, M.J., 2013. Major contribution of diatom resting spores to vertical flux in the sub-polar North Atlantic. Deep-Sea Res. Part I Oceanogr. Res. Pap. 82, 60–71. https://doi.org/10.1016/j.dsr.2013.07.013.

Salter, I., Kemp, A.E.S., Moore, C.M., Lampitt, R.S., Wolff, G.A., Holtvoeth, J., 2012. Diatom resting spore ecology drives enhanced carbon export from a naturally iron-fertilized bloom in the Southern Ocean. Global Biogeochem. Cycles 26. https://doi.org/10.1029/2010GB003977.

Sanders, R.J., Henson, S.A., Martin, A.P., Anderson, T.R., Bernardello, R., Enderlein, P., Fielding, S., Giering, S.L.C., Hartmann, M., Iversen, M., Khatiwala, S., Lam, P., Lampitt, R.S., Mayor, D.J., Moore, M.C., Murphy, E., Painter, S.C., Poulton, A.J., Saw, K., Stowasser, G., Tarling, G.A., Torres-Valdes, S., Trimmer, M., Wolff, G.A., Yool, A., Zubkov, M., 2016. Controls over ocean mesopelagic interior carbon storage (COMICS): fieldwork, synthesis, and modelling efforts. Front. Mar. Sci. 3, 136. https://doi.org/10.3389/fmars.2016.00136.

Sarmiento, J.L., Toggweiler, J.R., Najjar, R.P., 1988. Ocean carbon-cycle dynamics and atmospheric pCO2. Philos. Trans. R. Soc. London, Ser. A 325, 3–19. https://doi.org/10.1098/rsta.1988.0039.

Smetacek, V., Klaas, C., Strass, V.H., Assmy, P., Montresor, M., Cisewski, B., Savoye, N., Webb, A., d'Ovidio, F., Arrieta, J.M., Bathmann, U., Bellerby, R., Berg, G.M., Croot, P., Gonzalez, S., Henjes, J., Herndl, G.J., Hoffmann, L.J., Leach, H., Losch, M., Mills, M.M., Neill, C., Peeken, I., Röttgers, R., Sachs, O., Sauter, E., Schmidt, M.M., Schwarz, J., Terbrüggen, A., Wolf-Gladrow, D., 2012. Deep carbon export from a Southern Ocean iron-fertilized diatom bloom. Nature 487, 313–319. https://doi.org/10.1038/nature11229.

Thorpe, S.E., Heywood, K.J., Brandon, M.A., Stevens, D.P., 2002. Variability of the southern antarctic circumpolar current front north of South Georgia. J. Mar. Syst. 37, 87–105. https://doi.org/10.1016/S0924-7963(02)00197-5.

Villa-Alfageme, M., Briggs, N., Ceballos-Romero, E., de Soto, F., Manno, C., Giering, S.L., (this issue). Seasonal and Geographical Variations of Sinking Velocities in the Southern Ocean: Lessons Learned from COMICS I.

Ward, P., Atkinson, A., Venables, H.J., Tarling, G.A., Whitehouse, M.J., Fielding, S., Collins, M.A., Korb, R., Black, A., Stowasser, G., Schmidt, K., Thorpe, S.E., Enderlein, P., 2012. Food web structure and bioregions in the Scotia Sea: a seasonal synthesis. Deep Sea Res. Part II Top. Stud. Oceanogr. 59–60, 253–266. https://doi.org/10.1016/j.dsr2.2011.08.005.

Whitehouse, M.J., Priddle, J., Brandon, M.A., 2000. Chlorophyll/nutrient characteristics in the water masses to the north of South Georgia, Southern Ocean. Polar Biol. 23, 373–382. https://doi.org/10.1007/s003000050458.